Selective Growth and Integration of Silver Nanoparticles on Silver Nanowires at Room Conditions for Transparent Nano-Network Electrode

Haifei Lu, Di Zhang, Xingang Ren, Jian Liu, and Wallace C. H. Choy*

Department of Electrical and Electronic Engineering, The University of Hong Kong, Pokfulam Road, Hong Kong SAR, P.R. China

ABSTRACT Recently, metal nanowires have received great research interests due to their potential as next-generation flexible transparent electrodes. While great efforts have been devoted to develop enabling nanowire electrodes, reduced contact resistance of the metal nanowires and improved electrical stability under continuous bias operation are key issues for practical applications. Here, we propose and demonstrate an approach through a low-cost, robust, room temperature and room atmosphere process to fabricate a conductive silver nano-network comprising silver nanowires and silver nanoparticles. To be more specific, silver nanoparticles are selectively grown and chemically integrated *in situ* at the junction where silver nanowires meet. The site-selective growth of silver nanoparticles is achieved by a plasmon-induced chemical reaction using a simple light source at very low optical power density. Compared to silver nanowire electrodes without chemical treatment, we observe tremendous conductivity improvement in our silver nano-networks, while the loss in optical transmission is negligible. Furthermore, the silver nano-networks exhibit superior electrical stability under continuous bias operation compared to silver nanowire electrodes formed by thermal annealing. Interestingly, our silver nano-network is readily peeled off in water, which can be easily transferred to other substrates and devices for versatile applications. We demonstrate the feasibly transferrable silver conductive nano-network as the top electrode in organic solar cells. Consequently, the transparent and conductive silver nano-networks formed by our approach would be an excellent candidate for various applications in optoelectronics and electronics.

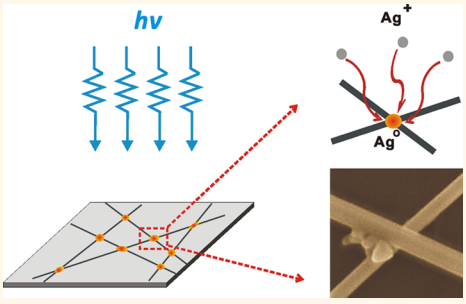

KEYWORDS: transparent electrode · silver nanowires · silver nanoparticles · nano-network · plasmon-induced chemical reaction

Transparent electrodes have been widely used in various technologies such as light display technologies, "smart" windows, and photovoltaic devices. Despite tin-doped indium oxide (ITO) being one of the most common materials for transparent electrodes, increasing concerns emerge because of its brittle property and the rare element of indium.[1,2] Consequently, novel transparent electrodes with features of low cost, high transmission, and good conductivity are highly desirable.[3−16] Randomly distributed metallic nanowires, which allow optical transparency and good conductivity as well as mechanical flexibility, have become an attractive alternative for flexible transparent electrodes.[13,17−24] In addition to the good optical and electrical properties, metallic nanowire electrodes also have the potential for low-cost production and large-scale solution-based processes.

Besides optimizing the length/diameter ratio, density, and distribution of silver nanowires on substrates for good optical transmittance and sheet resistance,[17,25−28] reducing the junction resistance between silver nanowires is one of the major directions to improve the electrical conductivity of the transparent electrode. Thermal annealing is generally adopted to reduce the junction resistance, whereas there is a concern about using the thermal annealing method for silver nanowires on flexible substrates, as the substrate may deform upon heating. Mechanical pressing and electroplating of gold have been reported to fuse Ag nanowire junctions, which help to decrease the sheet resistance and surface roughness of the films.[29] However, because of

* Address correspondence to chchoy@eee.hku.hk.

Received for review September 3, 2014 and accepted October 6, 2014.

Published online October 06, 2014
10.1021/nn504969z

the relatively large optical loss of gold, electroplated gold material on the silver nanowire surface would affect the optical absorption and transparency of the electrodes. Employing additional materials onto the silver nanowires, such as graphene, graphene oxide, PEDOT:PSS, metal oxide sol–gel, and nanoparticles, to achieve a composite transparent electrode, will at the same time alter the work function of the silver nanowire electrodes.[24,30−40] It is reported that a light-induced plasmonic nanowelding technique can assemble the silver nanowires into interconnected networks.[41] Typically, a light source with a very high optical power density of approximately 30 W/cm^2, which is about 300 times stronger than a one sun power density (=AM1.5G, 100 mW/cm^2), is required for the process. Such high optical power would be an issue for their application in large-scale electrode fabrication due to safety concerns, power consumption, and cost.

Here, we propose and demonstrate a novel approach of selective nucleation and growth of silver nanoparticles at the junctions of silver nanowires at room temperature and atmosphere to chemically form a silver nano-network. The selective integration of silver nanoparticles at the junctions of silver nanowires is realized through plasmon-induced chemical growth under a very low power density of light irradiation (as low as 5 mW/cm^2) without using sophisticated equipment and expensive material. As a result, silver nano-networks with very good electrical conductivity and optical transmittance are obtained. Compared to the silver nanowire electrodes treated with thermal annealing, our nano-networks from the selective integration of *in situ*-grown silver nanoparticles with silver nanowires exhibit better electrical stability under continuous external bias. In addition, the silver conductive nano-network peels itself off of the substrate when immersed in water, which can be easily transferred to other substrates for versatile applications. The transparent and conductive nano-network has been demonstrated as an efficient top electrode organic solar cell. Consequently, a silver nano-network formed through our novel approach has exhibited great potential as a highly conductive transparent electrode with attractive features of low cost and high operational stability, which are desirable in practical optoelectronic and electronic applications.

RESULTS AND DISCUSSION

Formation of the Silver Nano-Networks and Their Optical/Electrical Properties. The selective growth of silver nanoparticles at the junction of silver nanowires is achieved by illuminating the dispersed silver nanowires preformed on a substrate, which is immersed in aqueous solution of silver nitrate and sodium citrate. The sheet resistance of as-dispersed silver nanowire films is too large to be measured with a four-point probe approach, even after annealing at 100 °C for 10 min. The large sheet resistance can be mainly attributed to the huge contact resistance of silver nanowires. To effectively reduce the resistance between the nanowires, we employ a plasmon-induced chemical reaction which can selectively nucleate and grow silver nanoparticles *in situ* at the junctions of the silver nanowires. Silver nitrate and sodium citrate are chosen as the silver ion source and the reduction agent, respectively, and the silver nanowire acts as a catalyst for the plasmon-induced chemical reaction.[42,43] Under the illumination of visible light, a giant electric field can be strictly confined at the junction region due to plasmonic resonance. The chemically reduced silver atoms would subsequently deposit on the surface of silver nanowires at the junction region, which further induces the selective nucleation and growth of silver nanoparticles. The giant electric field obtained at around the crossed silver nanowires with different spacing has also been theoretically configured, as shown Supporting Information Figure S1. As a result, we find that the light with low optical power density can effectively activate the plasmon-induced chemical reaction and chemically reduce the silver ions at crosses of the silver nanowires. Consequently, the selective *in situ* growth of silver nanoparticles at the junctions of nanowires will bridge the contact, which is otherwise impossible for efficient current flow, and significantly reduce the contact resistance.

The experiments have been carried out as described in detail in the Methods section. An LED lamp (with an emission peak at 450 nm and an optical power density of 30 mW/cm^2) was initially selected to irradiate the sample for a specific duration. In order to obtain the optimal performance of the conductive nano-networks, we first investigated the electrical and optical properties of the silver nanowire films treated with different silver nitrate concentrations while keeping the concentration of sodium citrate under the illumination of the LED lamp for the same duration (10 min). As shown in Figure 1a, all the samples after the plasmon-induced chemical treatment present a drastic decrease of their sheet resistance compared to the silver nanowire electrodes without the treatment, of which the sheet resistance is huge. Meanwhile, their diffused transmittance shows a slight decrease, which can be attributed to the incorporation of silver nanoparticles in the nanowire films. As evidenced by the inset spectra of transmission change shown in Figure 1a, which is plotted by subtracting the transmission spectra of silver nanowire films treated by different silver nitrate concentrations from their corresponding untreated silver nanowire electrodes, the localized surface plasmon of the silver nanoparticles with a clear resonance peak at around 450 nm implies the presence of silver nanoparticles in the network. Although silver nanowire electrodes treated with aqueous solutions containing 1.2 and 2.0 mM silver nitrate show low sheet

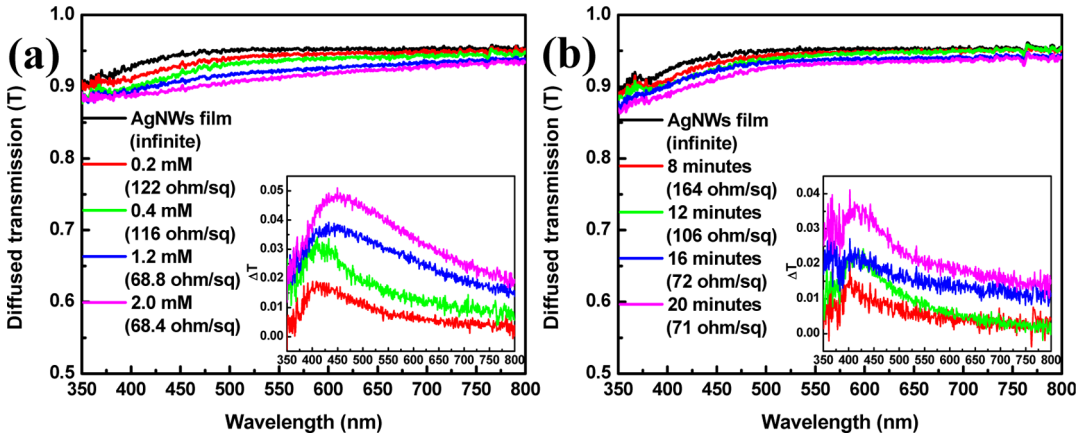

Figure 1. (a) Diffused transmission spectra of samples after the plasmon-induced chemical treatment at different concentrations of silver nitrate for the same duration. (b) Diffused transmission spectra of samples after the chemical treatment (using 0.2 mM silver nitrate) for different duration. Their sheet resistances after the chemical treatment are presented in the figures. Inset spectra are the transmission differences (ΔT) between silver NW films before and after plasmon-induced chemical treatment.

resistance, their optical transmittance decreases gradually with increasing silver nitrate concentration. While high optical transmission and low sheet resistance will be preferred for the application of transparent electrodes, we use the solution containing low silver concentration (0.2 mM) for the next step of optimization.

Silver nanowire films treated by varying light illumination durations have been also characterized as shown in Figure 1b. A sheet resistance of 72 ohm/sq has been obtained from the silver conductive nano-network after 16 min illumination, and the diffused transmittance at 550 nm shows only about 1.5% reduction. The further illumination will decrease the optical transmission, while less sheet resistance variation of the silver nanowire films has been observed. Therefore, a series of optimized silver conductive nano-networks with different surface coverage have been achieved, and their optical transmission spectra and sheet resistance are shown in Figure S2 and Table 1, respectively. The sheet resistances of the samples before the plasmon-induced chemical treatment are also provided. Our result shows that a silver conductive nano-network with an optical transmittance of 89.4% and a sheet resistance of 14.9 ohm/sq is achieved, which is comparable to that of commercial ITO film, while the silver conductive nano-network has the advantage of mechanical flexibility.

Figure 2a,b presents the scanning electron microscopy (SEM) image of silver nanowire films before and after our proposed plasmon-induced chemical treatment. Without any post-treatment, the conductivity between the silver nanowires is greatly confined by the incomplete contact between Ag nanowires and their relatively small contact area because of their round cross section. Interestingly, by adopting the plasmon-induced chemical reaction and nucleation strategy, silver nanoparticles form at junction regions of silver

TABLE 1. Optical Transmittances and Sheet Resistances of the Silver Nano-Network before and after the Plasmon-Induced Chemical Treatment

	silver NW electrodes (AFTER the plasmon-induced chemical treatment)		silver NW electrodes (BEFORE the plasmon-induced chemical treatment)
sample number	optical transmittance (at 550 nm)	sheet resistance (ohm/sq)	sheet resistance (ohm/sq)
1	94.8	469.3	∞
2	94.3	228.3	∞
3	93.2	54.9	147225
4	91.5	31.7	87202.5
5	90.4	21.9	36579.7
6	89.7	20.8	31483.5
7	89.4	14.9	12865.2
8	88.7	13.4	2787.3
ITO	89.5	19.6	

nanowires, as shown in the enlarged SEM images in Figure 2c,d, as well as indicated by the red arrows in Figure 2b. A transmission electron microscopy (TEM) image shown in Figure 1e further confirms the existence of silver nanoparticles. Hence, the selective introduction of silver nanoparticles into the cross regions of silver nanowires will increase the contact area between silver nanowires and eventually integrate the silver nanoparticles and silver nanowires as a highly conductive nano-network. Compared to other approaches, such as photothermal generation of silver nanowire welding, which needs high optical power density because of the poor photothermal conversion efficiency, very low power density of light irradiation is needed in our approach for the silver nanoparticle nucleation and growth. As a reference, when the silver nanowire electrode without any

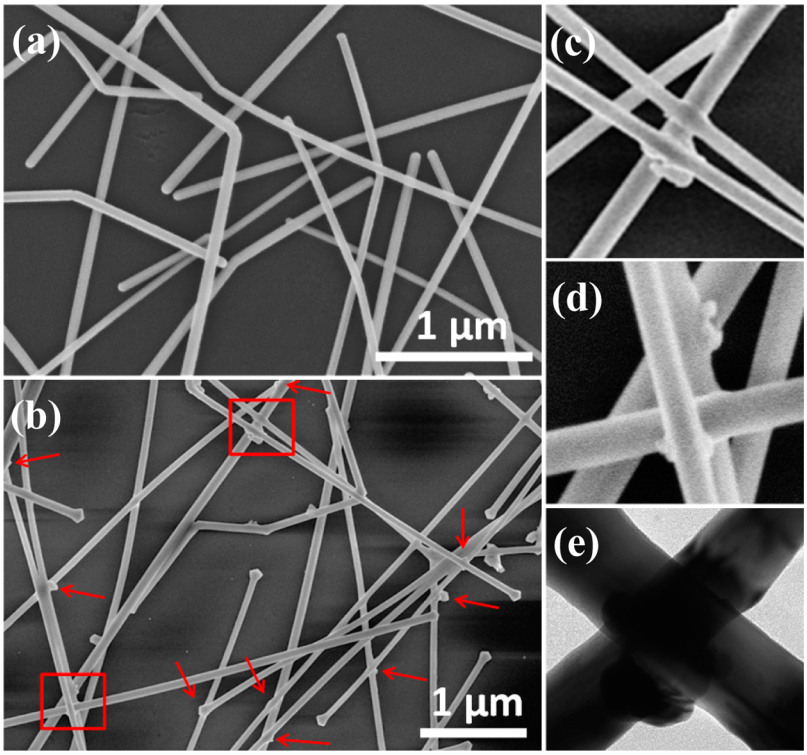

Figure 2. SEM images of silver nano-networks (a) before and (b) after the plasmon-induced chemical treatment. (c,d) Enlarged images indicated by the red squares in (b). (e) TEM image indicating the presence of a silver nanoparticle at the cross of silver nanowires.

treatment is exposed to the same LED lamp for a long time (*e.g.*, 1 h), the sheet resistance remains very high.

Furthermore, the LED lamp with different optical power densities, such as 40, 30, 20, 10, and 5 mW/cm^2, has also been demonstrated for the plasmon-induced chemical formation of the silver conductive nano-networks by varying the irradiation time. This implies that the higher the optical power density of the light source, the shorter the time required for forming a silver conductive nano-network with optimal performance. In addition, since a wide wavelength range of light is capable of generating a strong electric field between silver nanowires, such as the simulation result shown in Figure S1, LED lamps with different peak emissions at 475, 505, and 535 nm and other lamps having broadband emission wavelength, such as a sun simulator and a halogen lamp, have been used for demonstrating the plasmon-induced chemical process. The results indicate that our approach can be processed even using the daily sunlight as a light source.

Stable and Easily Transferrable Silver Nano-Network Electrode. The stability of the silver nano-network electrodes with and without plasmon-induced chemical treatment has been studied under a continuously external electrical bias. Besides our plasmon-induced chemically treated silver nano-network electrodes, four silver nanowire electrodes with identical nanowire density are also fabricated for comparison studies and are thermally annealed at different temperatures of 150, 180, 200, and 220 °C. Electrical contacts are formed at the two opposite ends of each sample electrode by using silver paste. In the resistance measurement, an electrical power density of 0.5 W/cm^2 is applied between the two silver paste contacts which allows the dc current to flow through the samples. The variations of their resistances under a constant external voltage bias have been measured.

For silver nanowires without any treatment (neither thermal nor chemical), the electrical contact between nanowires is considerably limited, which results in very large initial resistance of the electrodes. Thermal annealing treatment promotes the welding of nanowires at certain junctions, which contributes to the reduction of contact resistance. As shown in Figure 3, for thermally treated nanowire electrodes, increasing the annealing temperature from 150 to 220 °C leads to a noticeable reduction of the electrode resistance. However, under continuous electrical bias during which the Joule heating effect becomes prominent, the electrical stability of the thermally annealed nanowires becomes a serious issue. As shown in the inset of Figure 3, for nanowires annealed at relatively low temperatures of 150 and 180 °C, the resistance rapidly decreases initially due to the generated heat fusing the nanowires, thereby increasing the effective contact area (similar to thermal annealing effect).[44,45] Nevertheless, intensive Joule heating is primarily focused on a limited number of nanowire junctions with low resistance,

where heat cannot be effectively dissipated. The building up of heat quickly leads to the breakdown of nanowires, as shown in Figure S3, which further results in the rapid increase of resistance within the following several minutes. With higher annealing temperatures of 200 and 220 °C, more conductive junction regions are formed, which facilitates better heat dissipation and slower Joule heating. Indeed, the resistance of these electrodes shows no considerable changes during the first 20 min. Despite the improvement, the nanowires eventually break down within ~30 min. Differently, for our silver nano-network electrodes, the bridging of silver nanowires by the selective growth of nanoparticles creates significantly more conductive junction regions uniformly distributed across the electrode. Therefore, Joule heating is more evenly distributed, and little intensive heat accumulation is observed in the silver nano-networks, even after ~17 h of continuous operation (Figure 3). Consequently, the conductive silver nano-networks formed from our approach exhibit greatly enhanced electrical stability compared to thermally annealed nanowires, which can contribute to more stable performance in various devices using silver nanowires.

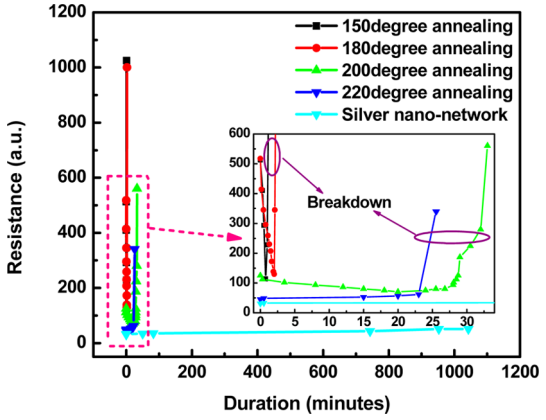

Figure 3. Resistance of silver nanowire electrodes prepared by thermal annealing at different temperatures and our nano-network under continuous external electrical bias.

Besides reducing the sheet resistance, the solution-based plasmon-induced chemical treatment will make the silver conductive nano-network hydrophobic due to the removal of remaining surfactant (polyvinylpyrrolidone) during the process, which is an essential material for the synthesis of silver nanowires. As shown in Figure 4a, the conductive nano-network will detach from the glass substrate when it is immersed into water and float on the water surface. Therefore, our conductive nano-network can be directly and easily transferred to other substrates without any other complicated transferring steps such as the case of graphene,[3,5] and no further postprocess after transfer is needed for achieving highly transparent and conductive electrode. In Figure 4b, the conductive nano-network has been demonstrated to be transferrable to a PET substrate. The flexibility of the conductive nano-network has been demonstrated in Figure S4, where less resistance variation of the conductive nano-network before and after bending has been observed. Hence, our transferable flexible conductive nano-network favors the applications in electronic and optoelectronic devices.

To conceptually demonstrate the potential application of our silver nano-network, semitransparent P3HT:PCBM organic solar cells (OSCs) were fabricated by using ITO and a silver nano-network as the bottom and top electrodes, respectively. The silver nano-network was first transferred to a PDMS film and then laminated on the OSC device. A reference opaque device had been fabricated by replacing the silver nano-network

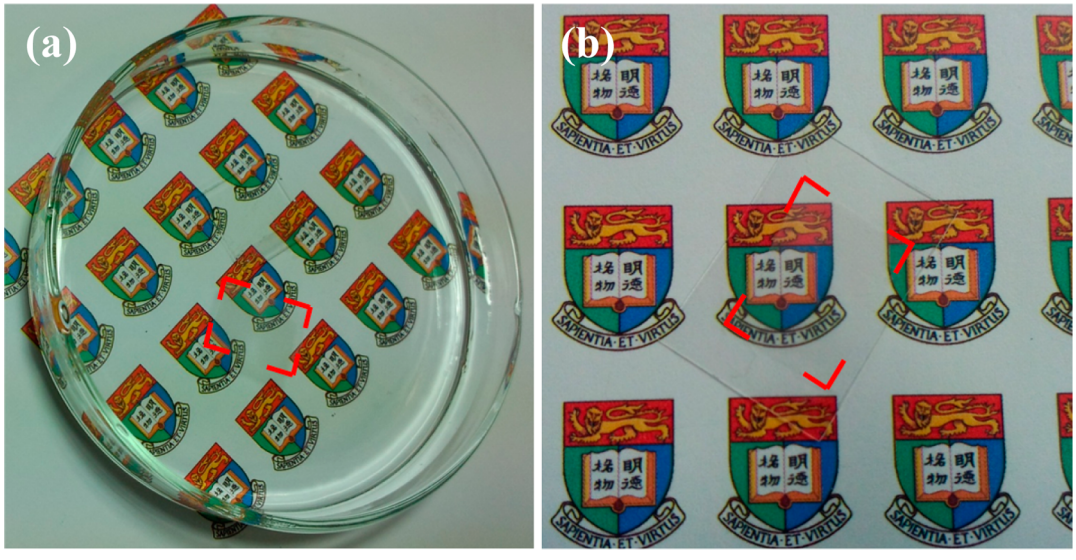

Figure 4. Photographs of our transparent and conductive silver nano-network (a) floating on water surface and (b) after transferred to a PET substrate. University of Hong Kong logo used with permission.

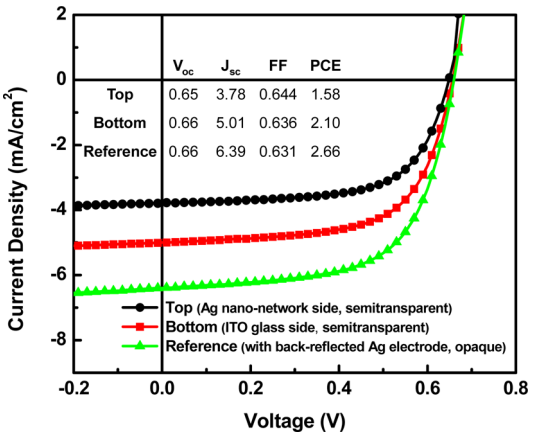

Figure 5. *J*–*V* characteristics of semitransparent P3HT:PCBM solar cell under AM1.5G illumination at 100 mW cm^{-2} from bottom (ITO glass) and top (silver nano-network) sides. The opaque reference device has been fabricated by replacing the silver nano-network with thermally evaporated silver film.

with thermally evaporated silver film. The details of device fabrication are described in the Methods section. As shown in Figure 5, the open circuit voltage (V_{oc}) and fill factor (FF) of the semitransparent OSC with the silver nano-network are similar to the standard opaque reference OSC, which indicates the good electrical contact between our silver nano-network and the interface layer underneath. In addition, similar values of V_{oc} and FF have been obtained by illuminating both sides of the semitransparent OSCs, that is, the bottom (ITO side) and top (silver conductive nano-network side). The difference in short circuit current density (J_{sc}) between the bottom and the top illumination can be attributed to the encapsulation of the device, which will induce loss of light approaching the top of the active layer due to the reflection and absorption of the glass slide, PDMS, and epoxy layers. The relatively weaker light from the top illumination will also reduce the V_{oc} device performance slightly as indicated in the table of Figure 5.[46] Consequently, the application of a silver nano-network as the top transparent electrode for semitransparent OSCs has been demonstrated.

CONCLUSION

In conclusion, a novel approach has been proposed and demonstrated to selectively grow and chemically integrate silver nanoparticles *in situ* onto the junctions of silver nanowires at room temperature and atmosphere for the formation of transparent and conductive silver nano-networks. The site-selective silver nanoparticles, grown through the plasmon-induced chemical reaction, can effectively enlarge the contact area at the junction of silver nanowires and make chemical integration of the silver nanowires so that the contact resistance decreases. We also demonstrate that light sources with different emission wavelengths and optical power densities can be employed for the plasmon-induced chemical growth of site-selective silver nanoparticles. Interestingly, owing to a more effective contact of silver nanowires achieved by the site-selective silver nanoparticles and the uniform distribution of heat generation under continuous external electrical bias, the conductive nano-network prepared from our approach exhibits much more stable performance than the silver nanowire electrodes formed by thermal annealing. Uniquely, our silver nano-network will peel off from the substrate in aqueous solution and can be easily transferred to other substrates and device surfaces. A conceptual demonstration of the application of our silver nano-network as the top electrode for semitransparent OSCs has been presented. Consequently, a silver nano-network formed by our novel approach with the advantages of reduced sheet resistance, improved operational stability, and the ability to be easily transferable will further advance the applications of low-cost, high-throughput electric and optoelectronic devices.

METHODS

Silver Nano-Network Formation. Silver nanowires with 100 nm average diameter were synthesized according previous literature[47] and washed with acetone and ethanol three times before being dispersed into ethanol with proper concentration. Different amounts of silver nanowire solution had been spin-coated on clean glass substrates for the formation of silver nanowire films with different densities. In order to selectively grow silver nanoparticles, the substrate with a silver nanowire film was immersed into an aqueous solution containing silver nitrate and sodium citrate and illuminated by visible light. Light from LED lamps with different emission, such as 450, 475, 505, and 535 nm, and light sources with wideband emission, such as a halogen lamp and sun simulator (AM1.5G), had been adopted here. After suitable irradiation duration, the substrate was taken out from the solution and blown with N_2 gas to remove the remaining aqueous solution.

Device Fabrication. To fabricate semitransparent OSCs, ITO glass substrates were cleaned by detergent and rinsed in deionized water, which were subsequently cleaned by acetone and ethanol. The precleaned substrates were then treated by ultraviolet/ozone for 15 min. Anatase phase TiO_2 nanocrystal solution was synthesized according to our previous reports[5,48] and was spin-coated onto ITO substrates, forming a ~20 nm thick electron transport layer. The prepared substrates were transferred into a nitrogen-filled glovebox for spin-coating the blend of poly(3-hexylthiophene) (P3HT) and [6,6]-phenyl-C61-butyric acid methyl ester ($PC_{61}BM$) with 10:8 weight ratio dissolved in chlorobenzene (10 mg/mL for P3HT and 8 mg/mL for $PC_{61}BM$). Once the polymer blend was dried, all the samples were thermally annealed at 130 °C for 5 min on a hot plate. PEDOT:PSS (Baytron AI 4083) doped with surfactant Triton X-100 from Aldrich (0.2% volume ratio) was spin-coated onto the polymer blend at 2000 rpm in ambient conditions. To fabricate top electrodes, a floating silver conductive nano-network was lifted off from water by soft polydimethylsiloxane (PDMS)/PET substrates. To form intimate contact between the top network electrode and the active layer, an electrically conductive glue, D-sorbitol, was added into the same Triton-doped PEDOT:PSS, and the PEDOT solution was then

spin-coated onto the NW/PDMS/PET stack at 2000 rpm.[49] Afterward, the nano-network top electrode stack and the substrate with polymer blend were brought into contact by a thermal lamination approach.[3] Before the lamination process, the more rigid PET (compared to PDMS) was peeled off from the network/PDMS to form a better contact. After the lamination process, the device was encapsulated by epoxy with a glass slide on top and cured under UV light. For the opaque reference device, the same processes as described above had been used except for the top silver electrode (100 nm), which was thermally evaporated at a pressure of 10^{-6} Torr.

Material and Device Characterizations. Scanning electron microscopy images were obtained using Hitachi S-4800 FEG and LEO 1530 FEG scanning electron microscopes. Transmission electron microscopy images were obtained using a FEI Tecnai G2 20 S-TWIN scanning transmission electron microscope. The sheet resistances of the electrodes were directly characterized by a standard four-point probe measurement approach, and diffused transmission spectra were obtained from a home-built optics system. Current density−voltage (*J*−*V*) characteristics were measured by using a Keithley 2635 sourcemeter and ABET AM1.5G solar simulator.

Conflict of Interest: The authors declare no competing financial interest.

Acknowledgment. This study was supported by the University Grant Council of the University of Hong Kong (Grants 10401466 and 201111159062), the General Research Fund (Grants HKU711813 and HKU711612E), an RGC-NSFC grant (N_HKU709/12), the Collaborative Research Fund (Grant CUHK1/CRF/12G) from the Research Grants Council of Hong Kong Special Administrative Region, China, and Grant CAS14601 from the CAS-Croucher Funding Scheme for Joint Laboratories.

Supporting Information Available: Additional SEM images, transmission spectra, and simulation results. This material is available free of charge *via* the Internet at http://pubs.acs.org.

REFERENCES AND NOTES

1. Hecht, D. S.; Hu, L. B.; Irvin, G. Emerging Transparent Electrodes Based on Thin Films of Carbon Nanotubes, Graphene, and Metallic Nanostructures. *Adv. Mater.* **2011**, *23*, 1482–1513.
2. Ellmer, K. Past Achievements and Future Challenges in the Development of Optically Transparent Electrodes. *Nat. Photonics* **2012**, *6*, 808–816.
3. Lin, P.; Choy, W. C. H.; Zhang, D.; Xie, F. X.; Xin, J. Z.; Leung, C. W. Semitransparent Organic Solar Cells with Hybrid Monolayer Graphene/Metal Grid as Top Electrodes. *Appl. Phys. Lett.* **2013**, *102*, 113303.
4. Kang, M. G.; Kim, M. S.; Kim, J. S.; Guo, L. J. Organic Solar Cells Using Nanoimprinted Transparent Metal Electrodes. *Adv. Mater.* **2008**, *20*, 4408–4413.
5. Zhang, D.; Xie, F. X.; Lin, P.; Choy, W. C. H. Al-TiO_2 Composite-Modified Single-Layer Graphene as an Efficient Transparent Cathode for Organic Solar Cells. *ACS Nano* **2013**, *7*, 1740–1747.
6. van de Groep, J.; Spinelli, P.; Polman, A. Transparent Conducting Silver Nanowire Networks. *Nano Lett.* **2012**, *12*, 3138–3144.
7. Chen, R. Y.; Das, S. R.; Jeong, C.; Khan, M. R.; Janes, D. B.; Alam, M. A. Co-Percolating Graphene-Wrapped Silver Nanowire Network for High Performance, Highly Stable, Transparent Conducting Electrodes. *Adv. Funct. Mater.* **2013**, *23*, 5150–5158.
8. Han, B.; Pei, K.; Huang, Y. L.; Zhang, X. J.; Rong, Q. K.; Lin, Q. G.; Guo, Y. F.; Sun, T. Y.; Guo, C. F.; Carnahan, D.; *et al.* Uniform Self-Forming Metallic Network as a High-Performance Transparent Conductive Electrode. *Adv. Mater.* **2014**, *26*, 873–877.
9. Bae, S.; Kim, H.; Lee, Y.; Xu, X. F.; Park, J. S.; Zheng, Y.; Balakrishnan, J.; Lei, T.; Kim, H. R.; Song, Y. I.; *et al.* Roll-to-Roll Production of 30-Inch Graphene Films for Transparent Electrodes. *Nat. Nanotechnol.* **2010**, *5*, 574–578.
10. Wu, H.; Kong, D. S.; Ruan, Z. C.; Hsu, P. C.; Wang, S.; Yu, Z. F.; Carney, T. J.; Hu, L. B.; Fan, S. H.; Cui, Y. A Transparent Electrode Based on a Metal Nanotrough Network. *Nat. Nanotechnol.* **2013**, *8*, 421–425.
11. Li, J.; Hu, L.; Wang, L.; Zhou, Y.; Gruner, G.; Marks, T. J. Organic Light-Emitting Diodes Having Carbon Nanotube Anodes. *Nano Lett.* **2006**, *6*, 2472–2477.
12. Zhang, D. Q.; Wang, R. R.; Wen, M. C.; Weng, D.; Cui, X.; Sun, J.; Li, H. X.; Lu, Y. F. Synthesis of Ultralong Copper Nanowires for High-Performance Transparent Electrodes. *J. Am. Chem. Soc.* **2012**, *134*, 14283–14286.
13. Rathmell, A. R.; Nguyen, M.; Chi, M. F.; Wiley, B. J. Synthesis of Oxidation-Resistant Cupronickel Nanowires for Transparent Conducting Nanowire Networks. *Nano Lett.* **2012**, *12*, 3193–3199.
14. Zou, J.; Li, C. Z.; Chang, C. Y.; Yip, H. L.; Jen, A. K. Interfacial Engineering of Ultrathin Metal Film Transparent Electrode for Flexible Organic Photovoltaic Cells. *Adv. Mater.* **2014**, *26*, 3618–3623.
15. Betancur, R.; Romero-Gomez, P.; Martinez-Otero, A.; Elias, X.; Maymo, M.; Martorell, J. Transparent Polymer Solar Cells Employing a Layered Light-Trapping Architecture. *Nat. Photonics* **2013**, *7*, 995–1000.
16. Sergeant, N. P.; Hadipour, A.; Niesen, B.; Cheyns, D.; Heremans, P.; Peumans, P.; Rand, B. P. Design of Transparent Anodes for Resonant Cavity Enhanced Light Harvesting in Organic Solar Cells. *Adv. Mater.* **2012**, *24*, 728–732.
17. De, S.; Higgins, T. M.; Lyons, P. E.; Doherty, E. M.; Nirmalraj, P. N.; Blau, W. J.; Boland, J. J.; Coleman, J. N. Silver Nanowire Networks as Flexible, Transparent, Conducting Films: Extremely High DC to Optical Conductivity Ratios. *ACS Nano* **2009**, *3*, 1767–1774.
18. Lee, J. Y.; Connor, S. T.; Cui, Y.; Peumans, P. Solution-Processed Metal Nanowire Mesh Transparent Electrodes. *Nano Lett.* **2008**, *8*, 689–692.
19. Chen, C. C.; Dou, L. T.; Zhu, R.; Chung, C. H.; Song, T. B.; Zheng, Y. B.; Hawks, S.; Li, G.; Weiss, P. S.; Yang, Y. Visibly Transparent Polymer Solar Cells Produced by Solution Processing. *ACS Nano* **2012**, *6*, 7185–7190.
20. Guo, H. Z.; Lin, N.; Chen, Y. Z.; Wang, Z. W.; Xie, Q. S.; Zheng, T. C.; Gao, N.; Li, S. P.; Kang, J. Y.; Cai, D. J.; *et al.* Copper Nanowires as Fully Transparent Conductive Electrodes. *Sci. Rep.* **2013**, *3*, 2323.
21. Sanchez-Iglesias, A.; Rivas-Murias, B.; Grzelczak, M.; Perez-Juste, J.; Liz-Marzan, L. M.; Rivadulla, F.; Correa-Duarte, M. A. Highly Transparent and Conductive Films of Densely Aligned Ultrathin Au Nanowire Monolayers. *Nano Lett.* **2012**, *12*, 6066–6070.
22. Yun, S.; Niu, X. F.; Yu, Z. B.; Hu, W. L.; Brochu, P.; Pei, Q. B. Compliant Silver Nanowire−Polymer Composite Electrodes for Bistable Large Strain Actuation. *Adv. Mater.* **2012**, *24*, 1321–1327.
23. Liang, J. J.; Li, L.; Niu, X. F.; Yu, Z. B.; Pei, Q. B. Elastomeric Polymer Light-Emitting Devices and Displays. *Nat. Photonics* **2013**, *7*, 817–824.
24. Lee, P.; Lee, J.; Lee, H.; Yeo, J.; Hong, S.; Nam, K. H.; Lee, D.; Lee, S. S.; Ko, S. H. Highly Stretchable and Highly Conductive Metal Electrode by Very Long Metal Nanowire Percolation Network. *Adv. Mater.* **2012**, *24*, 3326–3332.
25. De, S.; King, P. J.; Lyons, P. E.; Khan, U.; Coleman, J. N. Size Effects and the Problem with Percolation in Nanostructured Transparent Conductors. *ACS Nano* **2010**, *4*, 7064–7072.
26. Mutiso, R. M.; Sherrott, M. C.; Rathmell, A. R.; Wiley, B. J.; Winey, K. I. Integrating Simulations and Experiments To Predict Sheet Resistance and Optical Transmittance in Nanowire Films for Transparent Conductors. *ACS Nano* **2013**, *7*, 7654–7663.
27. Zhu, S. W.; Gao, Y.; Hu, B.; Li, J.; Su, J.; Fan, Z. Y.; Zhou, J. Transferable Self-Welding Silver Nanowire Network as High Performance Transparent Flexible Electrode. *Nanotechnology* **2013**, *24*, 335202.
28. Bergin, S. M.; Chen, Y. H.; Rathmell, A. R.; Charbonneau, P.; Li, Z. Y.; Wiley, B. J. The Effect of Nanowire Length and

Diameter on the Properties of Transparent, Conducting Nanowire Films. *Nanoscale* **2012**, *4*, 1996–2004.
29. Hu, L. B.; Kim, H. S.; Lee, J. Y.; Peumans, P.; Cui, Y. Scalable Coating and Properties of Transparent, Flexible, Silver Nanowire Electrodes. *ACS Nano* **2010**, *4*, 2955–2963.
30. Lee, J.; Lee, P.; Lee, H. B.; Hong, S.; Lee, I.; Yeo, J.; Lee, S. S.; Kim, T. S.; Lee, D.; Ko, S. H. Room-Temperature Nanosoldering of a Very Long Metal Nanowire Network by Conducting-Polymer-Assisted Joining for a Flexible Touch-Panel Application. *Adv. Funct. Mater.* **2013**, *23*, 4171–4176.
31. Woo, J. S.; Han, J. T.; Jung, S.; Jang, J. I.; Kim, H. Y.; Jeong, H. J.; Jeong, S. Y.; Baeg, K. J.; Lee, G. W. Electrically Robust Metal Nanowire Network Formation by *In-Situ* Interconnection with Single-Walled Carbon Nanotubes. *Sci. Rep.* **2014**, *4*, 4804.
32. Choi, D. Y.; Kang, H. W.; Sung, H. J.; Kim, S. S. Annealing-Free, Flexible Silver Nanowire–Polymer Composite Electrodes *via* a Continuous Two-Step Spray-Coating Method. *Nanoscale* **2013**, *5*, 977–983.
33. Choi, K. H.; Kim, J.; Noh, Y. J.; Na, S. I.; Kim, H. K. Ag Nanowire-Embedded ITO Films as a Near-Infrared Transparent and Flexible Anode for Flexible Organic Solar Cells. *Sol. Energy Mater. Sol. Cells* **2013**, *110*, 147–153.
34. Lee, J. H.; Shin, H. S.; Noh, Y. J.; Na, S. I.; Kim, H. K. Brush Painting of Transparent PEDOT/Ag Nanowire/PEDOT Multilayer Electrodes for Flexible Organic Solar Cells. *Sol. Energy Mater. Sol. Cells* **2013**, *114*, 15–23.
35. Chung, C. H.; Song, T. B.; Bob, B.; Zhu, R.; Yang, Y. Solution-Processed Flexible Transparent Conductors Composed of Silver Nanowire Networks Embedded in Indium Tin Oxide Nanoparticle Matrices. *Nano Res.* **2012**, *5*, 805–814.
36. Chen, T. L.; Ghosh, D. S.; Mkhitaryan, V.; Pruneri, V. Hybrid Transparent Conductive Film on Flexible Glass Formed by Hot-Pressing Graphene on a Silver Nanowire Mesh. *ACS Appl. Mater. Interfaces* **2013**, *5*, 11756–11761.
37. Zilberberg, K.; Gasse, F.; Pagui, R.; Polywka, A.; Behrendt, A.; Trost, S.; Heiderhoff, R.; Gorrn, P.; Riedl, T. Highly Robust Indium-Free Transparent Conductive Electrodes Based on Composites of Silver Nanowires and Conductive Metal Oxides. *Adv. Funct. Mater.* **2014**, *24*, 1671–1678.
38. Kim, A.; Won, Y.; Woo, K.; Jeong, S.; Moon, J. All-Solution-Processed Indium-Free Transparent Composite Electrodes Based on Ag Nanowire and Metal Oxide for Thin-Film Solar Cells. *Adv. Funct. Mater.* **2014**, *24*, 2462–2471.
39. Zhu, R.; Chung, C. H.; Cha, K. C.; Yang, W. B.; Zheng, Y. B.; Zhou, H. P.; Song, T. B.; Chen, C. C.; Weiss, P. S.; Li, G.; *et al.* Fused Silver Nanowires with Metal Oxide Nanoparticles and Organic Polymers for Highly Transparent Conductors. *ACS Nano* **2011**, *5*, 9877–9882.
40. Gaynor, W.; Burkhard, G. F.; McGehee, M. D.; Peumans, P. Smooth Nanowire/Polymer Composite Transparent Electrodes. *Adv. Mater.* **2011**, *23*, 2905–2910.
41. Garnett, E. C.; Cai, W. S.; Cha, J. J.; Mahmood, F.; Connor, S. T.; Christoforo, M. G.; Cui, Y.; McGehee, M. D.; Brongersma, M. L. Self-Limited Plasmonic Welding of Silver Nanowire Junctions. *Nat. Mater.* **2012**, *11*, 241–249.
42. Lu, H. F.; Zhang, H. X.; Yu, X.; Zeng, S. W.; Yong, K. T.; Ho, H. P. Seed-Mediated Plasmon-Driven Regrowth of Silver Nanodecahedrons (NDs). *Plasmonics* **2012**, *7*, 167–173.
43. Lu, H. F.; Kang, Z. W.; Zhang, H. X.; Xie, Z. L.; Wang, G. H.; Yu, X.; Zhang, H. Y.; Yong, K. T.; Shum, P.; Ho, H. P. Synthesis of Size-Controlled Silver Nanodecahedrons and Their Application for Core–Shell Surface Enhanced Raman Scattering (SERS) Tags. *RSC Adv.* **2013**, *3*, 966–974.
44. Nirmalraj, P. N.; Bellew, A. T.; Bell, A. P.; Fairfield, J. A.; McCarthy, E. K.; O'Kelly, C.; Pereira, L. F. C.; Sorel, S.; Morosan, D.; Coleman, J. N.; *et al.* Manipulating Connectivity and Electrical Conductivity in Metallic Nanowire Networks. *Nano Lett.* **2012**, *12*, 5966–5971.
45. Song, T. B.; Chen, Y.; Chung, C. H.; Yang, Y.; Bob, B.; Duan, H. S.; Li, G.; Tu, K. N.; Huang, Y.; Yang, Y. Nanoscale Joule Heating and Electromigration Enhanced Ripening of Silver Nanowire Contacts. *ACS Nano* **2014**, *8*, 2804–2811.
46. He, Z. C.; Zhong, C. M.; Su, S. J.; Xu, M.; Wu, H. B.; Cao, Y. Enhanced Power-Conversion Efficiency in Polymer Solar Cells Using an Inverted Device Structure. *Nat. Photonics* **2012**, *6*, 591–595.
47. Korte, K. E.; Skrabalak, S. E.; Xia, Y. N. Rapid Synthesis of Silver Nanowires through a $CuCl^{-}$ or $CuCl^{2-}$ Mediated Polyol Process. *J. Mater. Chem.* **2008**, *18*, 437–441.
48. Xie, F. X.; Choy, W. C. H.; Sha, W. E. I.; Zhang, D.; Zhang, S. Q.; Li, X. C.; Leung, C. W.; Hou, J. H. Enhanced Charge Extraction in Organic Solar Cells through Electron Accumulation Effects Induced by Metal Nanoparticles. *Energy Environ. Sci.* **2013**, *6*, 3372–3379.
49. Ouyang, H. Y.; Yang, Y. Conducting Polymer as Transparent Electric Glue. *Adv. Mater.* **2006**, *18*, 2141–2144.